Article

J. Biol. Regul. Homeost. Agents. 2022; 36(5): 1349–1358
https://doi.org/10.23812/j.biol.regul.homeost.agents.20223605.145

Transcriptomic Analysis of Neuropathic Pain in the Mouse Spinal Cord Following Peripheral Nerve Injury

Lili Jiang[1], Zhe Peng[2], Yuhui Deng[1], Peiyu Chen[1], Bingwei Yu[1], Miaosen Guo[1], Jinping Huang[1,*]

[1]Department of Anaesthesia, The Seventh Affiliated Hospital of Southern Medical University, 528000 Foshan, Guangdong, China
[2]Department of Anaesthesia, Foshan Women's and Children's Hospital Affiliated with Southern Medical University, 528000 Foshan, Guangdong, China
*Correspondence: 18923112869@189.cn (Jinping Huang)
Published: 20 October 2022

Background: Neuropathic pain (NP) is a chronic disease; Patients with NP most commonly seek treatment for primary or secondary injury of the peripheral or central nervous system. The complex pathophysiology of NP is not yet fully elucidated, which contributes to underassessment and undertreatment.
Methods: To analyse and study molecular relationships in the spinal cord in peripheral nerve induced neuropathic pain, we used SNI-induced neuropathic pain and Ribonucleic Acid (RNA) sequencing to analyse differ entially expressed genes (DEGs). We established an SNI (shared nerve injury) model and used third-generation transcriptome sequencing technology to analyse messenger Ribonucleic Acid (mRNA) expression in mouse SDH (spinal dorsal horn) tissue and obtained 325 differentially expressed genes. The differentially expressed genes were further analysed by bioinformatics analysis. A protein-protein interaction (PPI) network was constructed based on the STRING database, and Cytoscape software was used for visualization. We used the Kyoto Encyclopedia of Genes and Genomes (KEGG) pathway for DEGs to perform a Gene Ontology (GO) analysis. Real-time PCR (Polymerase Chain Reaction) was performed to verify the results.
Results: Atf3, Sprr1a, Anxa10, Ccl7, Ccl2, Lck, and Timp1 as well as the NF-κB TNF (Tumor Necrosis Factor) and MAPK (mitogen-activated protein kinase) signalling pathways, were implicated in SNI-induced neuropathicpain.
Conclusions: These findings further deepen the understanding of NP mechanisms and therapeutic targets.

Keywords: neuropathic pain; next generation sequencing; transcriptomes

Introduction

Neuropathic pain (NP) is the most challenging neuropathic pain in the world. It is mainly caused by damage to the peripheral or central nervous system or disease, which has a serious impact on the normal life of patients [1–3]. However, NP remains an elusive problem, and effective therapeutic approaches are still lacking because the specific mechanism of NP remains unclear. Therefore, it is urgent to further explore and confirm the underlying mechanism of NP and then develop related genes and signalling pathways to provide a theoretical basis for clinical treatment and find new paths.

The shared nerve injury (SNI) model can simulate the specific symptoms and treatment causes of neuropathic pain and is commonly used in neuropathic pain research. In recent years, driven by the development of Ribonucleic Acid sequencing (RNA-Seq) and bioinformatics technology, complete transcriptome analysis of gene changes has become possible [4,5]. RNA-Seq technology is currently used to characterize the transcriptome of the spinal cord under physiological conditions and to analyse genetic changes that occur during inflammation or neuropathic pain [6]. Third-generation Nanopore RNA sequencing technology can directly read the full-length sequences of high-quality individual RNA molecules from the 5′ end to the 3′ end polyA tail without interruption, accurately identify variable splicing (AS), selective polyadenylation (APA), fusion genes, and lncRNAs (long noncoding RNA) and their target genes that cannot be accurately identified by second-generation sequencing, and can also quantitatively analyse genes and transcripts simultaneously [7,8]. There have been many second-generation sequencing studies in neuropathic pain models, but there are still relatively few nanopore transcriptome sequencing studies on the mouse spinal cord. Because of the advantages of third-generation sequencing [9], we used nanopore technology to detect messenger Ribonucleic Acid (mRNA)in the spinal cord of SNI mice, performed bioinformatic analysis on the differentially expressed genes and performed partial validation to provide some insight for exploring the mechanism of neuropathic pain.

Journal of
BIOLOGICAL REGULATORS
and Homeostatic Agents

Methods

Animals

Male C57BL/6J mice weighing 20–25 g and aged 6–8 w were obtained from the Guangdong Provincial Medical Laboratory Animal Center. A total of 24 mice were allocated to the experiment, with 12 mice in each of the SNI and sham groups. Mice were placed in a standard laboratory at a temperature of 21 ± 1 °C for 12 hours each year. A 12-hour alternating cycle of day and night was maintained and food and water were not limited.

Establishment of the SNI Model

The neuropathic pain model induced by spared nerve injury (SNI) was constructed according to the procedure described by Decosterd [10]. Briefly, the mice were anaesthetized with isoflurane during the surgery. The left thigh was shaved, and the skin was disinfected with 75% alcohol and wiped dry. An incision was made in the outer epidermis of the mid-thigh. The biceps femoris was cut directly with scissors to ensure that the three terminal branches of the left tibial nerve, sciatic nerve, sural nerve, and common peroneal nerve could be fully exposed. The common peroneal and tibial nerves were secured with a small glass rod, ligated with 6-0 silk and transected at their ends, ensuring that 2–4 mm of each nerve was removed. Care was taken during the entire operation not to touch or stretch the intact sural nerve. Finally, each layer was suturedindividually using 5-0 silk.

Nociceptive Behaviour Test

All behavioural testing was conducted in a blinded manner. All mice were placed in the testing room for half an hour for three days prior to testing to acclimate to the testing environment. According to a previous article, von Frey hairs were used to analyse the sensitivity of the machine [11]. Briefly, using a brown plastic cylinder the mice were placed on a wire mesh table and habituated for 10 minutes. Von Frey filaments were applied to the outside of the rat's paw while the it was in a calm state, gradually increasing the von Frey hair from 0.04 g. The hair was shaped to an S shape, and the last 3 seconds of sudden paw withdrawal, withdrawal or paw licking behaviour was considered a positive reaction. If there were more than 3 positive reactions in 5 tests, this value was recorded, and an average of five round readings was calculated as the paw withdrawal mechanical threshold (PWMT).

Immunofluorescence Staining

Mice were anaesthetized first, placed under deep anaesthesia with sevoflurane, and then sequentially perfused with saline and 4% PFA (Paraformaldehyde) in their hearts. The samples were dehydrated in a gradient of sucrose solution (10%, 20%, 30%), and the lumbar spinal cord was divided into 20 μm thick slices using a cryostat (Leica). Multiplex immunofluorescence (IF) staining was performed under the guidance of standard protocols. Briefly, sections were placed in 0.3% Triton-100 buffer and kept blocked for one hour at room temperature and then incubated with primary antibody overnight at 4 °C (1:500, rabbit; Wako, Osaka, Japan). The sections were rinsed three times with PBS (Phosphate Buffered Saline) for 10 minutes each, and then incubated in horseradish peroxidase-conjugated secondary antibody (goat anti-rabbit IgG, Jackson ImmunoResearch, 1:1000, US) for 1 hour; Postwash section staining was performed uisng Alexa Fluor 594 Tyramide (Thermo Fisher, Waltham, MA, US). Finally, the stained sections were placed on glass slides and sealed with an anti-fluorescence quencher. The image source was a darkroom with a Leica scanning microscope (Olympus, Tokyo, Japan). Statistical analysis was performed using Image-Pro Plus 6.0 and GraphPad Prism 8, followed by inclusion analysis, and the mean optical density (AOD) was selected.

Total RNA Extraction

The mice were sacrificed under deep anaesthesia, and L4–6 spinal cords were collected, which were then placed in liquid nitrogen and frozen. Next, total RNA was extracted using the RNA prepPureTissue Kit (TianGen, Beijing, China). All apparatuses and reagents used in the experiment were Ribonuclease (RNase)-free.

RNA Sequencing

Total RNA (1 μg) was converted into a cDNA (complementary DNA) library according to the protocol given by Oxford Nanopore Technologies (ONT). Briefly, reverse transcription of full-length mRNA was performed using the SuperScript IV First Strand Synthesis System (Invitrogen, Waltham, MA, US), followed by 14 rounds of cDNA PCR (Polymerase Chain Reaction) using the LongAmp tag (NEB). The next step was to repair the FFPE DNA and end (NEB) of the PCR product, and the adapters were ligated with T4 DNA ligase (NEB). DNA purification was performed using Agencourt XP beads according to the ONT protocol. After the final cDNA library was pooled into the FLO-MIN109 flow cell, it was run on the PromethION platform at Biomarker Technology Company (Beijing, China).

Quantification of Gene/Transcript Expression Levels and Differential Expression Analysis

Full-length reads were mapped to reference transcriptome sequences. Reads with quality less than 5 were screened for quantification. Expression was estimated in terms of 10,000 mapped reads per gene or transcript. Analysis of differential expression between two groups was performed using the edgeRR package (3.8.6). The statistical routines provided by edgeR were combined with models based on the negative binomial distribution to identify differential expression in digital gene expression data. Ben-

jamini and Hochberg's role was to reduce the chance of error, and p values were obtained after further adjustment. Genes with an edgeR-derived p value < 0.05 and a fold change ≥ 1.5 were considered differentially expressed.

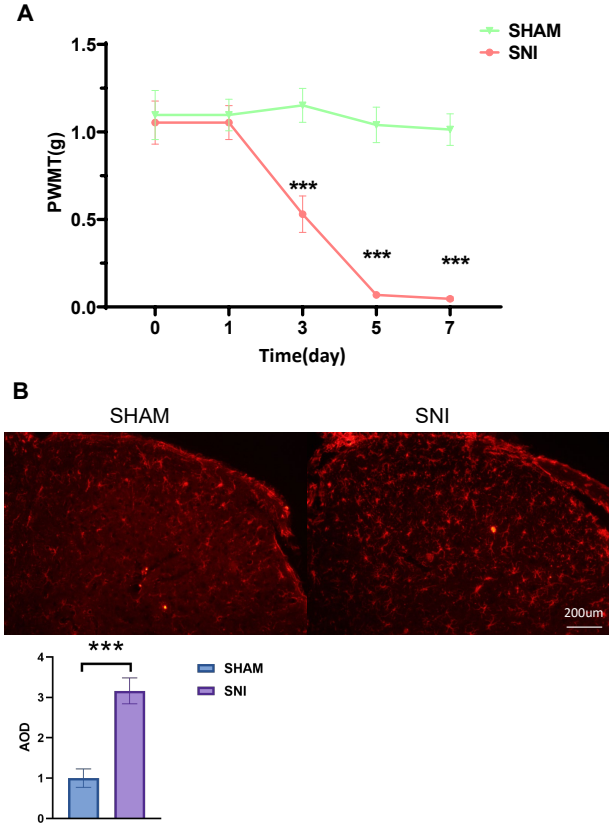

Fig. 1. Establishment of the neuropathic pain model. (A) Mechanical hyperalgesia was assessed using von Frey filaments. Compared with the sham-operated group, the paw withdrawal threshold showed a significant decreasing trend (red curve) on Days 3–7 after surviving nerve injury. Results were analysed by one-way analysis of variance (ANOVA) with multiple comparisons. $^{*}p < 0.05$, $^{**}p < 0.01$, and $^{***}p < 0.001$. (B) The marker of microglia, IBA1 (red), was significantly increased in the dorsal horn of the spinal cord in SNI mice. The average optical densities (AODs) in the images were quantified by ImageJ. The data are shown as the mean ± SEM (n = 3). The results were analysed by Student's t test. Spinal microglia are activated after SNI. Neuroinflammation plays an important role in neuropathic pain.

Functional Enrichment Analysis

GO Enrichment Analysis

Gene Ontology (GO) enrichment of differentially expressed genes (DEGs) was analysed using the Wallenius decentralized hypergeometric distribution of the GOseq (Gene Ontology analyser for RNA-seq) R package as a tool, with the ability to adjust gene length bias DEGs [12].

Table 1. Full-length sequence data statistics.

SampleID	Number of clean reads	Number of full-length reads	Full-Length Percentage
Control1	1,982,006	1,539,520	77.67%
Control2	1,848,368	1,429,326	77.33%
Control3	1,858,472	1,409,939	75.87%
Treat1	2,375,474	1,854,648	78.07%
Treat2	2,004,128	1,576,365	78.66%
Treat3	2,054,724	1,579,300	76.86%

Table 2. Clean reads and reference transcriptome comparison results.

Sample	Total Reads	Mapped reads	Mapped rates %
Control1	1,982,006	1,952,898	98.53%
Control2	1,848,368	1,819,707	98.45%
Control3	1,858,472	1,831,525	98.55%
Treat1	2,375,474	2,343,244	98.64%
Treat2	2,004,128	1,970,620	98.33%
Treat3	2,054,724	2,023,332	98.47%

KEGG Pathway Enrichment Analysis

As a database resource, Kyoto Encyclopedia of Genes and Genomes (KEGG) is based on molecular-level information, especially large-scale molecular datasets obtained by high-throughput experimental techniques such as genome sequencing, to further explore the advanced functions of cells, organisms and ecosystems (http://www.genome.jp/kegg/) [12]. In this study, the statistical enrichment test of differentially expressed genes in the KEGG pathway was completed with the help of KOBAS software (v2.0).

Protein-Protein-Interactions (PPIs)

The sequences of DEGs were blasted (blastx) into the genomes of related species (whose proteins interact and exist in the STRING database: http://string-db.org/), from which the predicted PPIs of these DEGs were obtained. Cytoscape was used to visualize PPIs of these DEGs [13].

GSEA

The identified genomes were analysed for prominent differences between groups by GSEA (http://www.broadinstitute.org/gsea/index.jsp). Lymph node and nonlymph node metastasis groups were analysed for mRNA expression levels, and a total of 24,991 were analysed. The normalized p value ($p < 0.05$) was used to filter out the function for further study [14].

Results

Nerve Injury Induced Neuropathic Pain in Mice

There was no difference in the paw withdrawal mechanical threshold (PWMT) between the control and SNI groups after three consecutive days of adaptation under

Journal of
BIOLOGICAL REGULATORS
and Homeostatic Agents

Table 3. The top ten genes with the largest differences.

Symbol	ID		Symbol	ID	
Atf3	ENSMUSG00000026628	up	Uncx	ENSMUSG00000029546	down
Sprr1a	ENSMUSG00000050359	up	Zfp873	ENSMUSG00000061371	down
Anxa10	ENSMUSG00000031635	up	Rdh9	ENSMUSG00000056148	down
Ccl7	ENSMUSG00000035373	up	Rpl36a-ps1	ENSMUSG00000060377	down
Ccl2	ENSMUSG00000035385	up	Mfap4	ENSMUSG00000042436	down
Lck	ENSMUSG00000000409	up	Gck	ENSMUSG00000041798	down
Lce1g	ENSMUSG00000027919	up	Egf	ENSMUSG00000028017	down
Oaf	ENSMUSG00000032014	up	Fam84b	ENSMUSG00000072568	down
Timp1	ENSMUSG00000001131	up	Acss3	ENSMUSG00000035948	down
Capn9	ENSMUSG00000031981	up	Ghsr	ENSMUSG00000051136	down

the same conditions. We next constructed a mouse model of surviving nerve injury (SNI) to present symptoms of chronic pain. The PWMT showed a significant decrease from the 3rd day after surgery compared with the control group and displayed allodynia, as the SNI mice showed a positive reaction to the minimum 0.04 g filament at the 7th day (Fig. 1A). The control group showed no significant difference at any time point. Spinal cord neuroinflammation is usually regarded as a prominent manifestation of neuropathic pain, and once Iba1 is activated in the dorsal horn of the spinal cord, spinal cord neuroinflammation develops (Fig. 1B). The above findings demonstrate that using a neuropathic pain model can establish surgery in SNI mice.

Transcripts Regulated the Spinal Cord of Mice after Peripheral Nerve Injury

We observed mice after SNI and then obtained transcriptome data from their spinal cords on Day 7 or in the control group using the RNA-seq method. The clean data output of each sample was 2.93 GB (Gigabyte), and each length of the sample had a sequence number ranging from 1848368 to 2375474 by identifying the total length of primer sequences at the ends of the reads (full length). The full-length percentage of each sample ranged from 75.87 to 78.66 (Table 1). Full-length sequenced transcriptomes and known transcriptomes were used to expand sequence alignments and provide references for further analysis. The sequence alignment of clean reads and the reference transcriptome was carried out with minimap2, and the corresponding information about the transcriptome and reference group was obtained, with a mapping rate percentage rate from 98.33 to 98.64 (Table 2). We tested the reliability of the gene expression level correlation experiments between samples and whether the selected samples meet key criteria. We computed between-sample correlation values based on the normalized expression results and drew correlation heatmaps (Fig. 2).

The purpose of DEG screening is to identify DEGs between samples and then carry out corresponding functional analysis. Fig. 3 details a representative distribution of up- or downregulated genes. According to the data, 7 days after

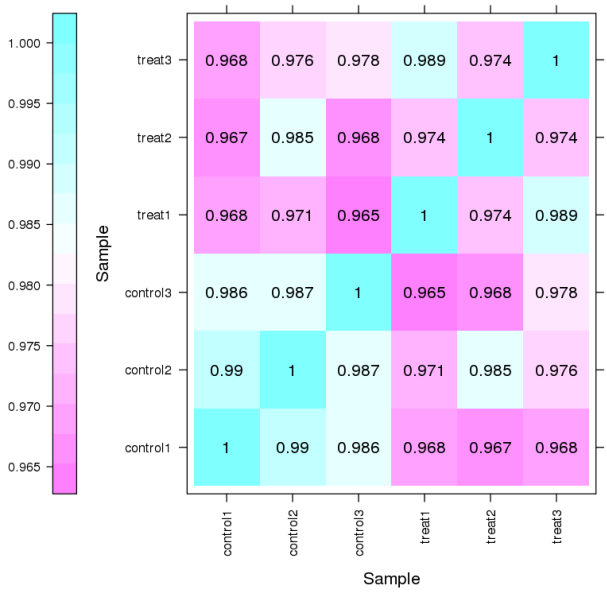

Fig. 2. Sample intersample correlation. The Pearson correlation coefficient r was used as an indicator to assess the biological replicate correlation. An r closer to 1 indicates that the two replicate samples are more correlated.

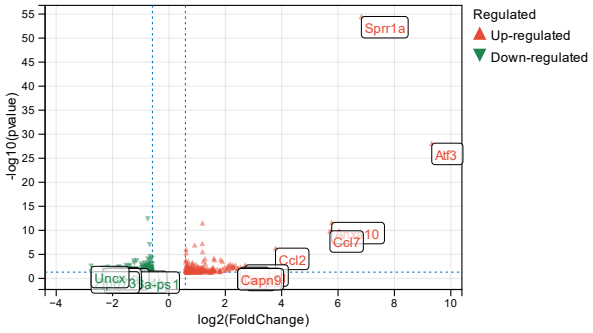

Fig. 3. Differential expression of volcanic maps. Volcano plots show how gene expression levels differ between two groups of samples, and whether the difference is statistically significant.

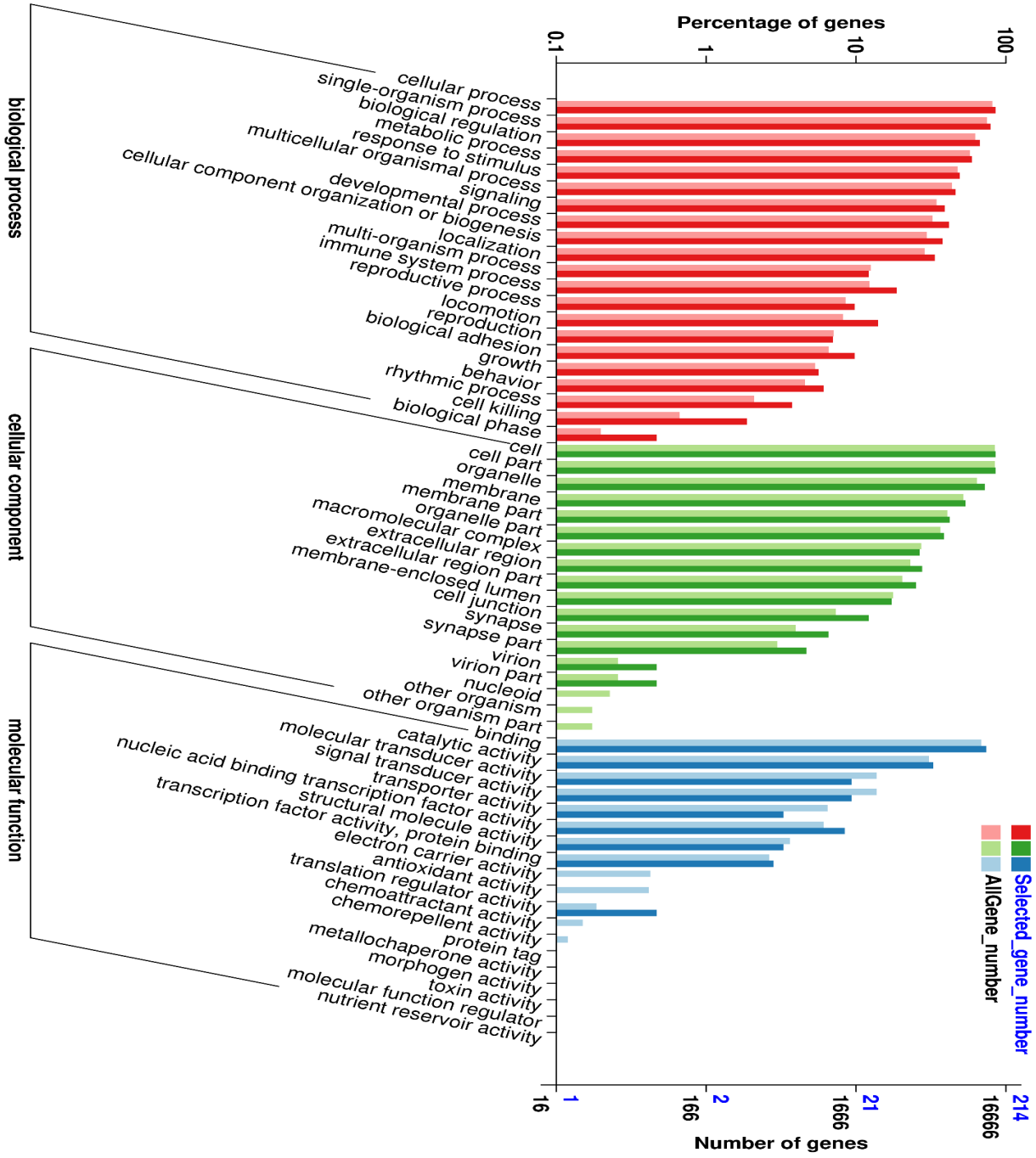

Fig. 4. The differences were expressed using the gene GO annotation classification chart. The GO annotation system mainly includes three important branches of biological process, molecular function and cellular components and is a directed acyclic graph.

SNI surgery, there were 185 upregulated genes in the mouse spinal cord, while the number of downregulated genes was 140. Up- and downregulated genes are represented by red and green dots, respectively. The top ten genes with the largest differences are listed in Table 3.

Pathway Analysis of DEGs in the SNI Model

To further explore the specific functions of DEGs in the mouse spinal cord after SNI surgery, Gene Ontology (GO) was further enriched and classified. GO analysis revealed an abundance of biological processes closely related to stimulus responses, biological regulation, immune system processes, and cell killing (Fig. 4). In addition, we analysed the differential genes in KEGG, and

Journal of
BIOLOGICAL REGULATORS
and Homeostatic Agents

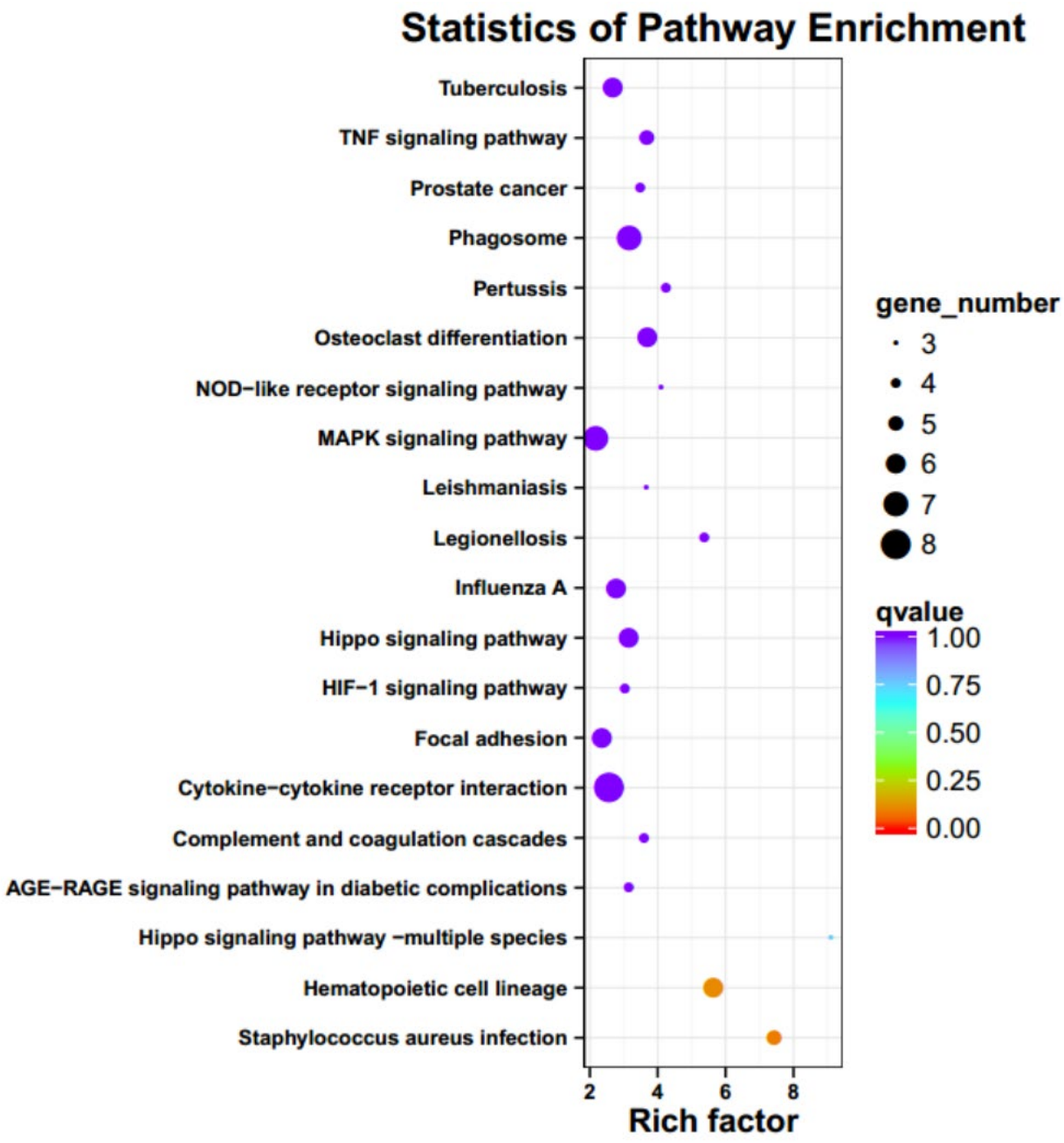

Fig. 5. Differences in gene expression in the gene KEGG channel enrichment point diagram. The figure shows the enrichment analysis results of the differentially expressed genes KEGG pathway, and the top 20 pathways of the series with the smallest significant Q value.

Fig. 5 shows the enrichment analysis results of differentially expressed transcripts and the KEGG pathway. We also screened the top 20 pathways with the smallest significant Q. These pathways include the TNF signalling pathway, MAPK signalling pathway, cytokine-cytokine receptor interaction, and Hippo signalling pathway, which are often identified in studies of neuropathic pain [15–18].

GSEA

To elucidate the molecular mechanism of SNI-induced neuropathic pain, KEGG and GSEA analyses were conducted. KEGG pathways enriched in the SNI group included herpes simplex virus 1 infection, glycan degradation, fat digestion and absorption, fructose and mannose metabolism, other glycan degradation and galactose metabolism (Fig. 5). In addition, the GSEA results are shown in (Fig. 6B).

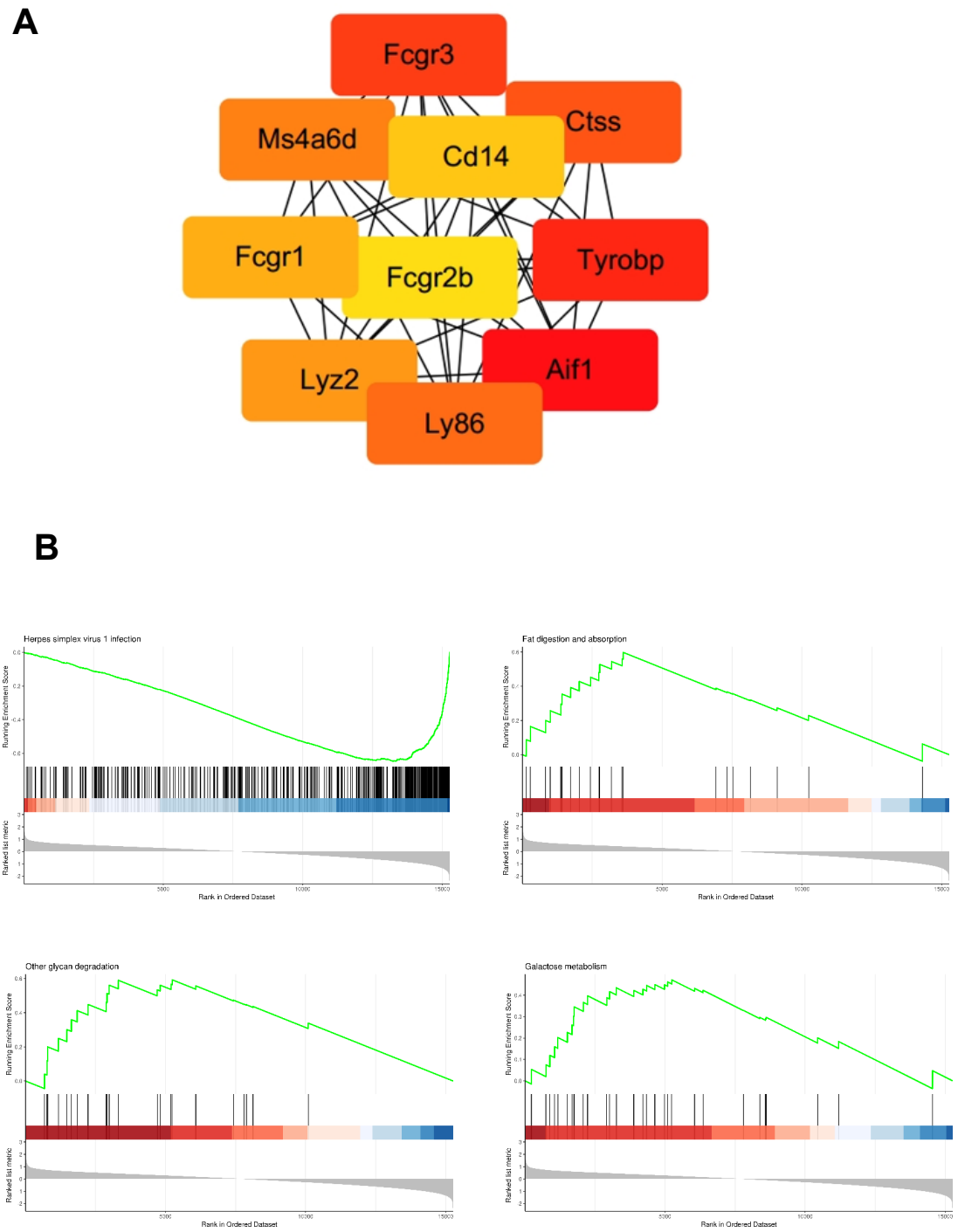

Fig. 6. Protein-protein interaction (PPI) and gene set enrichment analysis (GSEA) results. (A) Differences in expressesion in the gene-protein interaction network diagram. Using BLAST software (V2.1), the target transcripts were aligned with the protein sequences in the database, homologous proteins were identified, and a reciprocal network was built based on their reciprocal relationships. The constructed protein interaction network can be imported into Cytoscape software (Cytoscape 3.5.1) for visualization. (B) Gene set enrichment analysis result map. In this paper, in the process of GSEA, the gene sets of the KEGG pathway and the BP, CC, and MF branches of GO were used as the gene set of interest, and then the $\log_2$FC of each differential grouping was used as the score of the background gene set to complete the gene set of interest. Enrichment analysis of the set was performed, and finally, the controllable *p* value or FDR was the significantly enriched gene set. Here, we screened out the top 4 enriched GO nodes/pathways of the enrichment map based on the GSEA results: Herpes simplex virus 1 infection, glycan degradation, fat digestion and absorption, fructose and mannose metabolism, and other glycan degradation.

Journal of
BIOLOGICAL REGULATORS
and Homeostatic Agents

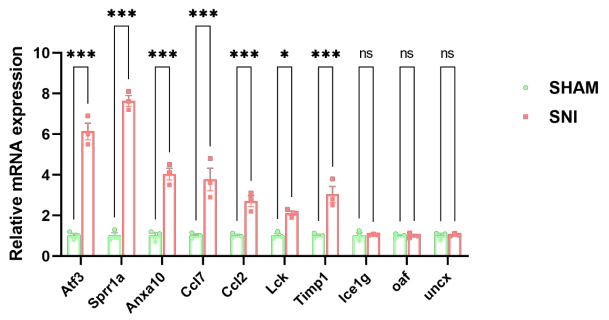

Fig. 7. Validation of target genes. qPCR was introduced to validate target genes in the dorsal horn of the spinal cord. The results were analysed by *T* test. $^{*}p < 0.05$, $^{**}p < 0.01$, and $^{***}p < 0.001$.

Table 4. Primer information.

Target name		Primer
Atf3	F	GAGGATTTTGCTAACCTGACACC
	R	TTGACGGTAACTGACTCCAGC
Sprr1a	F	TTGTGCCCCCAAAACCAAG
	R	GGCTCTGGTGCCTTAGGTTG
Anxa10	F	ATGTTTTGCGGGGAATATGTCC
	R	CAATCAGCATGTCTTTGTTGCAG
Ccl7	F	GCTGCTTTCAGCATCCAAGTG
	R	CCAGGGACACCGACTACTG
Ccl2	F	TTAAAAACCTGGATCGGAACCAA
	R	GCATTAGCTTCAGATTTACGGGT
Lck	F	TGGAGAACATTGACGTGTGTG
	R	ATCCCTCATAGGTGACCAGTG
Lce1g	F	GCTACCCTTCATATTGCTCCTGA
	R	CAGGCTACAGCAGGAAGACA
Oaf	F	AGCCAGGTGATCGAGGAGAG
	R	CCTTCTTGAAATCCGCGATGA
Timp1	F	GCAACTCGGACCTGGTCATAA
	R	CGGCCCGTGATGAGAAACT
Uncx	F	ACCCGCACCAACTTTACCG
	R	TGAACTCGGGACTCGACCA

Protein-Protein Interaction (PPI) Network Analysis

Through PPI analysis of 325 genes, we found that the deduced main hub genes were Aif1, Tyrobp, Fcgr3, Ctss, Ly86, Ms4a6d, Lyz2, Fcgr1, Cd14, and Fcgr2b (Fig. 6A).

qPCR Validation

qPCR was performed to validate the mRNA levels of the ten DEGs. Atf3, Sprr1a, Anxa10, Ccl7, Ccl2, Lck, Lce1 g, Oaf, Timp1, and Uncx. Atf3, Sprr1a, Anxa10, Ccl7, Ccl2, Lck, and Timp1 were found to be upregulated, supporting the sequencing analysis (Fig. 7, Table 4). The differences in lce1 g, oaf, and uncx in our qPCR validation were not statistically significant.

Discussion

It has been well established that the mechanism of NP generation and development, such as abnormal gene expression and activation of related pathways, is very complex [19,20]. It was recently observed that gene expression profiles also changed in the spinal cord after SNI. Therefore, it is essential to explore the mechanisms of NP at the genomic level. In this study, 325 DEGs were screened for more in-depth bioinformatics analysis, and genetic targets were identified for diagnosing and treating NP.

The top 10 most promising DEGs (including Atf3, Sprr1a, Anxa10, Ccl7, Ccl2, Lck, Lce1 g, Oaf, Timp1 and Uncx) affecting NP progression was derived from a comprehensive interpretation of differential gene expression in the spinal cord. Atf3 can be activated by a variety of signals and participates in multiple complex processes, including cellular stress responses. The finding of increased atf-3 mRNA in the spinal cord after nerve injury indicates that Atf3 is likely to be a candidate genetic marker affecting NP progression [21,22]. The expression of proline-rich small repeat protein 1A (Sprr1a) appears in the dorsal root ganglia (DRG) and spinal cord after peripheral nerve injury and was therefore used to assess the regenerative potential of damaged neurons [23]. Anxa10 (Annexin A10) [24,25] belongs to the annexin family, and its biological effects originate from calcium-dependent phospholipid binding and binding of calcium ions. Neuroinflammation by proinflammatory cytokines and chemokines, including ccl2 and ccl7, has been demonstrated to promote and maintain neuropathic pain [26]. As a member of the Src family, it has been confirmed that Lck has an important influence on the occurrence and development of neuropathic pain [27]. It was also demonstrated that Timp1 was associated with chronic pain after spinal cord injury but not with chemotherapy-induced peripheral neuropathy [28,29].

We then analysed these DEGs using various bioinformatics analysis methods and obtained a comprehensive analysis to provide insight into these genes. According to the KEGG enrichment analysis, DEGs were more enriched in the NF-κB pathway, TNF pathway and MAPK pathway, which may have significant effects on SNI-induced neuropathic pain. Previous research findings also confirmed this. Activation of the NF-κB pathway promotes the synthesis and release of proinflammatory cytokines such as TNF-α, IL-6, and IL-1β, which may have a major impact on the development of neuroinflammation, while activation of the MAPK pathway may regulate neuronal plasticity. Activation of the NF-κB pathway leads to the synthesis and release of proinflammatory cytokines, such as TNF-α, IL-6, and IL-1β, and activation of the MAPK pathway is likely to have an important impact on neuroinflammation [30]. Moreover, neuroinflammation is often associated with neuropathic pain. Therefore this pathology is relevant, as the pathways screened in the KEGG enrichment are closely associated with neuroinflammation [31–33].

DEG-enriched GO terms often included "response to stimulus", "biological regulation", "immune system process", and "cell killing". These results demonstrate the vital role of the stress response and immune system, consistent with previous studies [34,35]. Central sensitization is a nociceptive input that triggers long-term pain, but it increases the excitability of neurons in the central nociceptive pathway and the reversibility of synaptic ability, showing obvious pain hypersensitivity, especially abnormal pain caused by dynamic touch [36]. It can be used to express synaptic plasticity in the spinal cord and brain, increasing neuronal responses in central pain pathways after an initial painful stimulus. More evidence shows that neuroinflammation in the peripheral and central nervous systems similarly drives central sensitization. Activation of immune cells in the spinal cord and brain, such as microglia and astrocytes, is a prominent feature of neuroinflammation, which in turn releases proinflammatory cytokines and chemokines. Our findings show that astrocytes and microglia are activated in the spinal cord of mice with neuropathic pain, suggesting that immune cells play an important role in the development and progression of neuropathic pain.

Conclusions

In conclusion, the results of this experiment confirm that DEGs, such as Atf3, Sprr1a, Anxa10, Ccl7, Ccl2, Lck, and Timp1, as well as the NF-κB, TNF and MAPK signalling pathways, are involved in neuropathic pain caused by SNI. Our research provides solid evidence for the involvement of neuroinflammation in neuropathic pain from a bioinformatics perspective and provides a new direction for better clinical prevention or treatment of neuropathic pain.

Author Contributions

JH and LJ—designed the research study; LJ and ZP—performed the research; YD and PC—provided help and advice on the PCR experiments; BY and MG—analyzed the data. All authors contributed to editorial changes in the manuscript. All authors read and approved the final manuscript.

Ethics Approval and Consent to Participate

The above experiments strictly followed the relevant principles of the International Association for the Study of Pain and were submitted to the Animal Care and Use Committee of Southern Medical University for record and approval (2020068).

Acknowledgment

Not applicable.

Funding

This research received no external funding.

Conflict of Interest

The authors declare no conflict of interest.

References

[1] Finnerup NB, Kuner R, Jensen TS. Neuropathic Pain: From Mechanisms to Treatment. Physiological Reviews. 2021; 101: 259–301.
[2] Colloca L, Ludman T, Bouhassira D, Baron R, Dickenson AH, Yarnitsky D, *et al*. Neuropathic Pain. Nature Reviews Disease Primers. 2017; 3: 17002.
[3] Alles SRA, Smith PA. Etiology and Pharmacology of Neuropathic Pain. Pharmacological Reviews. 2018; 70: 315–347.
[4] Wang K, Wang S, Chen Y, Wu D, Hu X, Lu Y, *et al*. Single-cell transcriptomic analysis of somatosensory neurons uncovers temporal development of neuropathic pain. Cell Research. 2021; 31: 904–918.
[5] Stark R, Grzelak M, Hadfield J. RNA sequencing: the teenage years. Nature Reviews. Genetics. 2019; 20: 631–656.
[6] Wang K, Yi D, Yu Z, Zhu B, Li S, Liu X. Identification of the Hub Genes Related to Nerve Injury-Induced Neuropathic Pain. Frontiers in Neuroscience. 2020; 14: 488.
[7] Deamer D, Akeson M, Branton D. Three decades of nanopore sequencing. Nature Biotechnology. 2016; 34: 518–524.
[8] Reiner JE, Balijepalli A, Robertson JWF, Campbell J, Suehle J, Kasianowicz JJ. Disease Detection and Management via Single Nanopore-Based Sensors. Chemical Reviews. 2012; 112: 6431–6451.
[9] Petersen LM, Martin IW, Moschetti WE, Kershaw CM, Tsongalis GJ. Third-Generation Sequencing in the Clinical Laboratory: Exploring the Advantages and Challenges of Nanopore Sequencing. Journal of Clinical Microbiology. 2019; 58: e01315–e01319.
[10] Decosterd I, Woolf CJ. Spared nerve injury: an animal model of persistent peripheral neuropathic pain. Pain. 2000; 87: 149–158.
[11] Peng Z, Yang F, Huang S, Tang Y, Wan L. Targeting VEGFA with Soluble VEGFR1 Ameliorates Nerve Injury-Induced Neuropathic Pain. Molecular Pain. 2022; 17448069221094528. (online ahead of print)
[12] Young MD, Wakefield MJ, Smyth GK, Oshlack A. Gene ontology analysis for RNA-seq: accounting for selection bias. Genome Biology. 2010; 11: R14.
[13] Shannon P, Markiel A, Ozier O, Baliga NS, Wang JT, Ramage D, *et al*. Cytoscape: a Software Environment for Integrated Models of Biomolecular Interaction Networks. Genome Research. 2003; 13: 2498–2504.
[14] Subramanian A, Tamayo P, Mootha VK, Mukherjee S, Ebert BL, Gillette MA, *et al*. Gene set enrichment analysis: a knowledge-based approach for interpreting genome-wide expression profiles. Proceedings of the National Academy of Sciences. 2005; 102: 15545–15550.
[15] Sun W, Yang S, Wu S, Ba X, Xiong D, Xiao L, *et al.* Transcriptome analysis reveals dysregulation of inflammatory and neuronal function in dorsal root ganglion of paclitaxel-induced peripheral neuropathy rats. Molecular Pain. 2022; 17448069221106167. (online ahead of print)
[16] Lu J, Guo X, Yan M, Yuan X, Chen S, Wang Y, *et al*. P2X4R Contributes to Central Disinhibition via TNF-α/TNFR1/GABAaR Pathway in Post-stroke Pain Rats. The Journal of Pain. 2021; 22: 968–980.

[17] Kanngiesser M, Mair N, Lim H, Zschiebsch K, Blees J, Häussler A, *et al*. Hypoxia-Inducible Factor 1 Regulates Heat and Cold Pain Sensitivity and Persistence. Antioxidants & Redox Signaling. 2014; 20: 2555–2571.

[18] Li N, Lim G, Chen L, McCabe MF, Kim H, Zhang S, *et al*. Spinal expression of Hippo signaling components YAP and TAZ following peripheral nerve injury in rats. Brain Research. 2013; 1535: 137–147.

[19] Safieh-Garabedian B, Nomikos M, Saadé N. Targeting inflammatory components in neuropathic pain: the analgesic effect of thymulin related peptide. Neuroscience Letters. 2019; 702: 61–65.

[20] Sommer C, Leinders M, Üçeyler N. Inflammation in the pathophysiology of neuropathic pain. Pain. 2018; 159: 595–602.

[21] Hsieh Y, Kan H, Chiang H, Lee Y, Hsieh S. Distinct TrkA and Ret modulated negative and positive neuropathic behaviors in a mouse model of resiniferatoxin-induced small fiber neuropathy. Experimental Neurology. 2018; 300: 87–99.

[22] Hsieh Y, Chiang H, Lue J, Hsieh S. P2X3-mediated peripheral sensitization of neuropathic pain in resiniferatoxin-induced neuropathy. Experimental Neurology. 2012; 235: 316–325.

[23] Gaub P, Joshi Y, Wuttke A, Naumann U, Schnichels S, Heiduschka P, *et al*. The histone acetyltransferase p300 promotes intrinsic axonal regeneration. Brain. 2011; 134: 2134–2148.

[24] Sun L, Xu Q, Zhang W, Jiao C, Wu H, Chen X. The involvement of spinal annexin a10/NF-κB/MMP-9 pathway in the development of neuropathic pain in rats. BMC Neuroscience. 2019; 20: 28.

[25] Lu Y, Ni S, He L, Gao Y, Jiang B. Annexin a10 is involved in the development and maintenance of neuropathic pain in mice. Neuroscience Letters. 2016; 631: 1–6.

[26] Zhang Z, Jiang B, Gao Y. Chemokines in neuron-glial cell interaction and pathogenesis of neuropathic pain. Cellular and Molecular Life Sciences. 2017; 74: 3275–3291.

[27] Tsuda M, Tozaki-Saitoh H, Masuda T, Toyomitsu E, Tezuka T, Yamamoto T, *et al*. Lyn tyrosine kinase is required for P2X4 receptor upregulation and neuropathic pain after peripheral nerve injury. Glia. 2008; 56: 50–58.

[28] Tonello R, Lee SH, Berta T. Monoclonal Antibody Targeting the Matrix Metalloproteinase 9 Prevents and Reverses Paclitaxel-Induced Peripheral Neuropathy in Mice. The Journal of Pain. 2019; 20: 515–527.

[29] Sandhir R, Gregory E, He Y, Berman NEJ. Upregulation of Inflammatory Mediators in a Model of Chronic Pain after Spinal Cord Injury. Neurochemical Research. 2011; 36: 856–862.

[30] Chang S, Li X, Zheng Y, Shi H, Zhang D, Jing B, *et al.* Kaempferol exerts a neuroprotective effect to reduce neuropathic pain through TLR4/NF-κB signaling pathway. Phytotherapy Research: PTR. 2022; 36: 1678–1691.

[31] Ellis A, Bennett DLH. Neuroinflammation and the generation of neuropathic pain. British Journal of Anaesthesia. 2013; 111: 26–37.

[32] Matsuda M, Huh Y, Ji R. Roles of inflammation, neurogenic inflammation, and neuroinflammation in pain. Journal of Anesthesia. 2019; 33: 131–139.

[33] Walters SB, Kieckbusch J, Nagalingam G, Swain A, Latham SL, Grau GER, *et al*. Microparticles from Mycobacteria-Infected Macrophages Promote Inflammation and Cellular Migration. The Journal of Immunology. 2013; 190: 669–677.

[34] Grace PM, Tawfik VL, Svensson CI, Burton MD, Loggia ML, Hutchinson MR. The Neuroimmunology of Chronic Pain: From Rodents to Humans. The Journal of Neuroscience. 2021; 41: 855–865.

[35] Liu Y, Latremoliere A, Li X, Zhang Z, Chen M, Wang X, *et al*. Touch and tactile neuropathic pain sensitivity are set by corticospinal projections. Nature. 2018; 561: 547–550.

[36] Woolf CJ. Central sensitization: implications for the diagnosis and treatment of pain. Pain. 2011; 152: S2–S15.